

Local Structure at Mn Sites in Icosahedral Mn-Al Quasicrystals

E. A. Stern and Y. Ma

Department of Physics, University of Washington, Seattle, Washington 98195

and

C. E. Bouldin

Semiconductor Materials and Processes Division, National Bureau of Standards, Gaithersburg, Maryland 20899

(Received 8 July 1985)

Extended x-ray-absorption fine-structure measurements have been made at the Mn *K* edge of quasicrystalline and crystalline forms of an Al_6Mn alloy. Two different quasicrystalline Mn sites are discerned to be populated in the ratio of τ , the golden mean, within experimental error. The more populous site is similar to that in the crystal but with bond-angle distortions and elimination of an unusually short Al-Mn bond, while the other site has additional bond-stretching distortions. The measurements together with density measurements indicate that the volume per Mn site is independent of the type of site.

PACS numbers: 61.50.Em, 61.55.Hg, 64.60.My, 78.70.Dm

The recent discovery¹ of a rapidly cooled phase of Al_6Mn which has sharp diffraction peaks yet icosahedral rotational symmetry—a condition which is incompatible with crystalline order—has generated a spate of activity²⁻⁹ to explain these extraordinary results. Among other things, it has become clear that many different classes of models can, in principle, satisfy the general properties of these rapidly quenched quasicrystalline alloys. Incommensurate density modulation of a crystalline structure with one³ or more⁵ components, and a quasiperiodic translational order as a new class of order between crystalline and amorphous^{2,10,11} are some of the models proposed. In addition, within each class it is possible to discern subgroups which are analogous to simple cubic, face-centered-cubic, and body-centered-cubic structures. Finally, of course, the concept that a group of atoms should be associated with each point of the model structure must eventually be considered since, experimentally, the new class of materials has been found only in alloys with more than one type of atom present.

To obtain more insight into the constraints that are imposed by nature on any model, an extended x-ray-absorption fine-structure (EXAFS) study at the Mn *K* edge was made on quasicrystalline and crystalline forms of the alloy with nominal composition Al_6Mn (27 wt.% of Mn). Both samples were in powder form. The quasicrystalline form was prepared in such a manner as to minimize contamination with the Al-metal phase. The powder was further ground into a size finer than 400 mesh and then rubbed into the sticky side of Scotch brand Miracle tape. Two layers of the tape were used to obtain a sample with a Mn *K* edge of $\Delta\mu x \approx 0.4$. Measurements were made on the IV-1 beam line at the Stanford Synchrotron Radiation Laboratory with use of a (220) double-crystal Si monochromator, an electron beam energy of 3 GeV, and a

current ranging from 30 to 60 mA. The gases in the ion chambers were chosen and the double-crystal monochromator was detuned to minimize harmonic contamination. These precautions plus the uniformity of the sample thickness and its smallness all assure minimum distortion of the EXAFS amplitude by thickness effects.¹² Measurements were made at sample temperatures of 80 K, 180 K, and room temperature for both the quasicrystal and the crystal forms.

The data were analyzed in the standard fashion¹³ isolating the oscillatory EXAFS signal $\chi(k)$ normalized by the *K*-edge step. The wave number *k* is calculated in units of inverse angstroms by $k = [0.263(E - E_0)]^{1/2}$, where *E* is the absorbed x-ray-photon energy in electronvolts and E_0 is the zero of the energy scale taken about 12 eV below the edge so that at the edge the photoelectron *k* is equal to k_F , the free-electron value of the Fermi wave number. Figure 1 shows the $\chi(k)$ at 80 K for the quasicrystal and that of

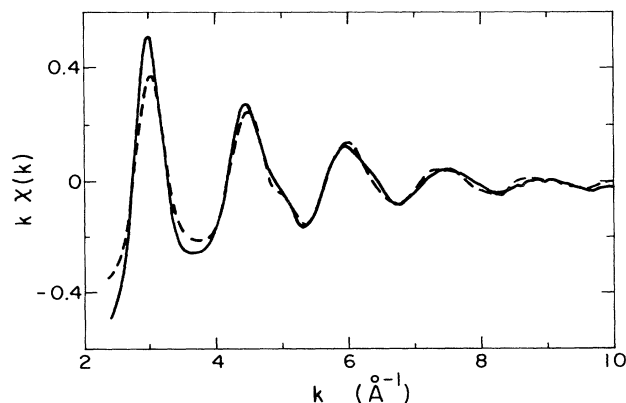


FIG. 1. A $k\chi(k)$ plot for the quasicrystal (solid line), and the crystal weighted by 0.618 (dashed line). Data were taken at 80 K.

the crystal weighted by $\tau^{-1} = \tau - 1 = 0.618$, where $\tau = (1 + \sqrt{5})/2$ is the golden mean. Note that for $k > 4 \text{ \AA}^{-1}$ the two signals are quite similar. In Fig. 2 the magnitudes of the Fourier transforms of the quasicrystal and the crystal forms are displayed. They correspond to the positions of coordination shells of atoms shifted by $\sim 0.5 \text{ \AA}$ as a result of phase-shift effects. Both transforms display two main peaks for $r < 5 \text{ \AA}$, although the crystal ones are larger. At larger r the crystal has a peak at $r = 6 \text{ \AA}$, and another at $\sim 7 \text{ \AA}$, both of which are significantly above the noise level and are missing in the quasicrystal. Various tests were to verify that the peaks at 6 and 7 \AA are real and not artifacts of the "cutoff wiggles" introduced by the windows used to limit the data range.

To analyze the differences between the crystal and the quasicrystal more quantitatively, the first shell in each was isolated and transformed back to k space. The amplitude and phase of the isolated shell were calculated for both forms, and the logarithm of the ratio of the amplitudes plotted versus k^2 are shown in Fig. 3. The change in slope from a significantly negative one to an approximately zero one is indicative of the contribution of two components.¹⁴ The initial negative slope is indicative of a site in the quasicrystal with more disorder in the Mn-Al bond distances than is present in the crystal, while the approximately zero slope belongs to a site whose Mn-Al bonds are very similar to those in the crystal. However, a significant difference in the third moment of the bond distances about the average, c_3 , was detectable through a k^3 term in the phase difference¹⁵ for the ordered sites, as can be noted in the high k range of Fig. 1. A comparison of the linear k terms in the phase indicates that the average Mn-Al distance for both sites in the quasicrystal was closely the same as that in the crystal.

The Al_6Mn crystal¹⁶ serves as a satisfactory standard for the quasicrystal. There are 4 Mn and 24 Al atoms per unit cell, but all Mn sites have the same environ-

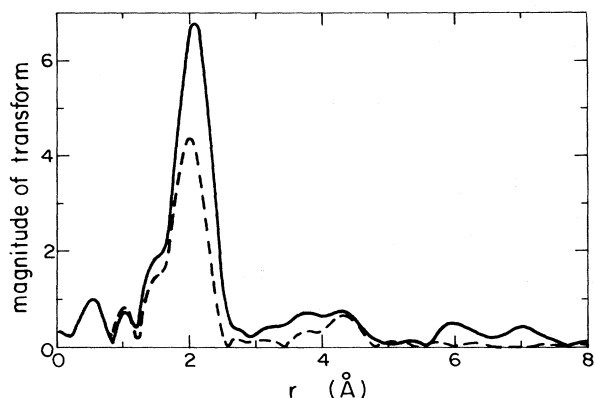


FIG. 2. The magnitude of the Fourier transform of $k^3\chi(k)$ over the range $2.5 \text{ \AA}^{-1} < k < 11.7 \text{ \AA}^{-1}$, for the crystal (solid line) and the quasicrystal (dashed line).

ment. The near-neighbor environment about the Mn is ten Al atoms at an average distance of 2.56 \AA with second, third, and fourth cumulants about this average of $\sigma^2 = 5.1 \times 10^{-3} \text{ \AA}^2$, $c_3 = -3.1 \times 10^{-4} \text{ \AA}^3$, and $C_4 = -1.7 \times 10^{-5} \text{ \AA}$, respectively. The second and third cumulants are equal to the second and third moments, while the fourth cumulant is equal to the fourth moment minus $3\sigma^4$. The logarithm of the ratio in Fig. 3 is not affected by C_4 since it is too small to contribute in the plotted k range, while the odd cumulant C_3 affects only the phase.¹⁵ Thus, in Fig. 3, the contribution of the crystal can be accurately approximated by a Debye-Waller factor $\exp(-2k^2\sigma^2)$.

The decomposition of the quasicrystal signal into the two components was done as follows. The contribution from the more-ordered component of the quasicrystal was eliminated by subtraction of a weighted crystal $\chi(k)$ from the quasicrystal one. The phase of the crystal's first-shell $\chi(k)$ was modified by addition of the k^3 term discerned in the phase difference and produced by the change in c_3 . The spectrum subtracted was Fourier transformed into r space and the weight and σ^2 adjusted so as to minimize the size of the first peak corresponding to the Mn-Al bonds. The weight obtained by this method gave 0.60 ± 0.05 and a third-moment difference between the quasicrystal and the crystal of $(7 \pm 2) \times 10^{-4} \text{ \AA}$. The average Mn-Al bond distance was the same within the experimental accuracy of 0.02 \AA and the difference in mean square disorder was $\Delta\sigma^2 = 0.0005 \pm 0.001 \text{ \AA}^2$. Note that it is not accurate to obtain the weight and $\Delta\sigma^2$ by extrapolation of the high- k slope in Fig. 3 to $k = 0$. The second site adds to the slope since its contribution is not negligible there.

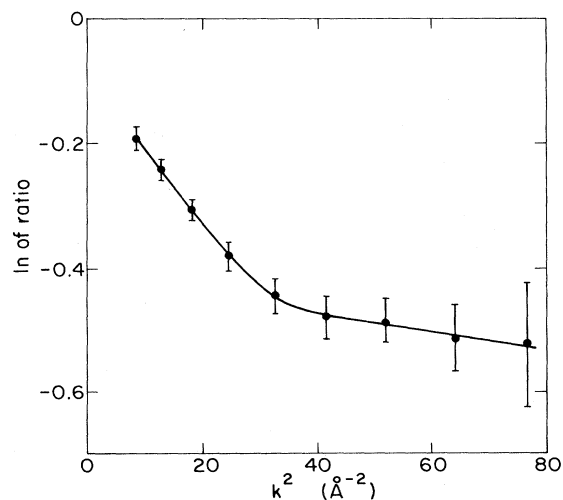


FIG. 3. The logarithm of the ratio of the amplitude of the inverse-transformed, isolated first shell of the quasicrystal divided by that of the crystal as a function of k^2 . The solid curve is a smooth line fitted by eye to the experimental points.

After isolation of the more-disordered component by subtraction, it was analyzed by the method¹³ using the logarithm of the ratio of amplitudes and the difference in phase to obtain the result that it consists of 0.37 ± 0.05 of the sample. This component is more disordered than the crystal is by $\Delta\sigma^2 = 0.033 \pm 0.003 \text{ \AA}^2$ and has an average Mn-Al bond which is, again, the same as that in the crystal with an uncertainty of 0.03 \AA . Because of its larger disorder, the phase difference in the more-disordered portion could not be discerned to large enough k values to determine the presence of a k^3 term. In obtaining the fraction of the quasicrystal sample taken up by each component, the assumption was made that there is the same number of Al neighbors in each as in the crystal, namely, ten. This assumption is reasonable for the ordered component since it is so similar in average Mn-Al bond distance and distribution about this average. The sum of the two components should be 1 if they both have ten Al neighbors to the Mn atoms. The sum, 0.9 ± 0.08 , is 1 within experimental error. Alternatively, the deficit from 1 could be interpreted as the disordered site having less than ten Al neighbors. In this interpretation the number of Al neighbors for this site would be 9 ± 1.3 .

It is also possible to fit Fig. 3 by two Gaussians. Within experimental error, such a fit obtains the same values for α and $\Delta\sigma^2$ as are obtained by the subtraction method described above. The subtraction method has the advantage of making fewer assumptions about the more-disordered site. That is, it does not assume that the site has only Gaussian broadening; instead, the result follows from the analysis.

As noted above, Fig. 2 shows a qualitative change between the quasicrystal and the crystal, namely, a lack of significant peaks beyond $r = 5 \text{ \AA}$ in the quasicrystal. The peak at $r = 6 \text{ \AA}$ in the crystal was analyzed further and was shown by its k dependence to be predominantly composed of Mn atoms. Normally, it is not possible to interpret peaks reliably at such large distances because they are obscured by multiple scatterings and interference between overlapping shells of atoms.¹⁵ However, this special case is an exception because Mn is so much heavier than Al and the Mn-Mn distances are so large. The Mn-Mn signal extends to higher k than that of the Mn-Al signal and can thus be separated. In addition, the Al atoms have a broad distribution at the larger distances and tend to cancel one another's EXAFS. Thus, in this case, only the Mn-Mn multiple scatterings might obscure the Mn-Mn signal. However, this does not occur because the Mn-Mn atoms are so far apart that their multiple scatterings are weak.¹⁷

The peak at $r = 4.4 \text{ \AA}$ due to the four Mn atoms at 4.98 \AA from the center Mn in the crystal is also identified as predominantly a Mn-Mn peak and its oc-

currence in both forms of the alloy indicate that the Mn environment has similar lengths up to that distance in the ordered portion of the quasicrystal. The abrupt disappearance of the Mn-Mn peaks that occurs beyond that distance cannot be understood as a discontinuity in this environment because then the Mn atoms at the surface would see a different environment, in disagreement with the experimental result that the nearest-neighbor environment is the same for all Mn atoms. The only viable explanation for the results is that the nearest-neighbor distances up to $\sim 5 \text{ \AA}$ are the same but the angles between these bonds are distorted in the quasicrystal. Distortions in the angles will change the more-distant atom positions, introducing a greater disorder in these distances and causing a disappearance of their peak in the transform.

To summarize the experimental results, there are two distinct Mn sites in the quasicrystal. Within experimental error, a fraction τ^{-1} of the Mn atoms populate the site which is similar to that in the crystal of Al_6Mn except for an increase of the third moment of the Mn-Al distances and distortion of their bonding angles. The second site, populated by $1 - \tau^{-1} = \tau^{-2}$ of the Mn atoms, is different from that in the crystal, having about the same average bonding length to the nearest Al neighbors but having more variation in that length by $\Delta\sigma^2 = 0.033 \pm 0.003 \text{ \AA}^2$. The coordination number at that site may be decreased by 1 ± 1.3 Al atoms. The ratio of the Mn atoms in the two sites is τ within an uncertainty of 8%.

Figure 3 indicates a bimodal distribution of Al atoms about the Mn, and we interpreted this in the most physically reasonable manner as indicating two Mn sites. However, EXAFS alone cannot completely rule out the possibility of a single Mn site with an unusual bimodal distribution of Al atoms. Recent Mössbauer results⁴ on the icosahedral phase $(\text{Fe}_x\text{Mn}_{1-x})_{1.03}\text{Al}_6$ indicate more than one Mn site, giving confirmation to our interpretation. When the Mössbauer results are interpreted in terms of two sites they also indicate a ratio of occupancy of τ within experimental error. The EXAFS results indicate how these two sites differ from one another and their relation to the crystal.

The results have implications for the structure of the quasicrystal and the understanding of why the quasicrystal seems to be limited to Al_6Mn -related structures. Besides the obvious requirement of a Mn-Al complex to be placed on each point of the structure, there are two different sites in the structure which distort the Mn-Al complex in different ways. It is tempting to associate these two sites with the two polyhedra that can be used in the three-dimensional Penrose tiling.^{2,10,11} The volumes of the polyhedra are in the ratio of τ , the same ratio of the two sites found by EXAFS. However, the frequencies of occurrence of the two polyhedra are also in the ratio of τ in such a

manner as to produce τ^2 more volume in the larger polyhedra than in the smaller. Although our measurements indicate that the average Mn-Al bond length is closely the same at the two sites and that the coordination number does not change drastically, this does not necessarily imply that the volume per Mn atom is the same at the two sites. For example, if the lines connecting Mn and Mn at the more-disordered sites are distorted to lie almost in a plane, the volume per atom can be made as small as desired. If the volume per Mn site were the same then the factor of τ would come from the different volumes of the polyhedra and their numbers would have to be equal, excluding a Penrose structure. However, if the more-disordered sites are distorted so that they occupy the smaller-volume polyhedra in the same number as the larger polyhedra, as suggested previously,⁴ the factor of τ would come from the frequency of occurrence of the polyhedra consistent with a Penrose-type structure.

The two possibilities can be distinguished by density measurements. The similarity of the ordered sites in the quasicrystal to those of the crystal indicates that the volume per Mn at these sites must be closely the same. The disordered site would then have to have a smaller volume in order to fit the same number of Mn atoms into the smaller polyhedra in order to be consistent with a Penrose-type structure. The corresponding Penrose-type quasicrystal would be 17% more dense than the crystal. Recent density measurements¹⁸ find that the quasicrystal have the same density within $\sim 3\%$, inconsistent with this model of a Penrose-type structure.

One of the questions to be answered is why the icosahedral quasicrystal phase is so rare, occurring only in a limited number of structures related to Al_6Mn . The EXAFS results give a tantalizing clue that may answer this question. The crystal Mn sites have a Mn-Al bond at 2.435 \AA , which is shorter than the average by 0.12 \AA , imposed by the symmetry requirements of the crystal structure.¹⁶ This produces an unusual negative sign to the third moment of the bond-length distribution about the average, c_3 . The increase in the third moment in the quasicrystal produces the more usual positive sign of c_3 by, presumably, elimination of the 2.435-\AA bond. This would enhance the relative stability of the icosahedral quasicrystal phase compared with the crystal since the unusually short Mn-Al bond must be energetically expensive. Finally, it has been recently suggested¹⁹ that the icosahedral phase may be closely related to the crystalline $\alpha(\text{AlMnSi})$ phase.²⁰ Our results show that this is not the case. The crystal has two different Mn sites as in the quasicrystal but in the wrong ratio of 1 to 1.

The EXAFS determination of the short-range environment about the Mn atoms is complementary in-

formation to that obtained from indexing x-ray and neutron diffraction scans of the quasicrystals which, when properly understood, should determine a structure of points about which the Mn-Al complex determined by EXAFS must be placed.

We greatly appreciate the very informative and stimulating conversations with J. W. Cahn, who also kindly supplied the quasicrystalline and crystalline forms of the sample. We are also pleased to acknowledge an informative discussion with Professor B. Grunbaum. One of us (C.E.B.) is a U. S. Nuclear Regulatory Commission postdoctoral fellow. The help of the staff at Stanford Linear Accelerator Center where the measurements were made is greatly appreciated. The Stanford Synchrotron Radiation Laboratory is supported by the U. S. Department of Energy, Office of Basic Energy Science, and the National Institutes of Health, Biotechnology Resource, Division of Research Resources.

¹D. Shechtman, I. Blech, D. Gratias, and J. W. Cahn, *Phys. Rev. Lett.* **53**, 1951 (1984).

²D. Levine and P. J. Steinhardt, *Phys. Rev. Lett.* **53**, 2477 (1984).

³P. Bak, *Phys. Rev. Lett.* **54**, 1517 (1985).

⁴L. J. Swartzendruber, D. Shechtman, L. Bendersky, and J. W. Cahn, *Phys. Rev. B* **32**, 1383 (1985).

⁵D. Mermin and S. M. Troian, *Phys. Rev. Lett.* **54**, 1524 (1985).

⁶P. A. Bancel, P. A. Heiney, P. W. Stephens, A. I. Goldman, and D. M. Horn, *Phys. Rev. Lett.* **54**, 2422 (1985).

⁷S. Sachdev and D. R. Nelson, unpublished.

⁸V. Elser, *Phys. Rev. Lett.* **54**, 1730 (1985).

⁹D. Devine, T. C. Lubensky, S. Ostlund, S. Tamaswamy, D. J. Steinhardt, and J. Toner, *Phys. Rev. Lett.* **54**, 1520 (1985).

¹⁰A. L. MacKay, *Physica* **114A**, 609 (1982), and *Kristallografiya* **26**, 910 (1981) [*Sov. Phys. Crystallogr.* **26**, 517 (1981)].

¹¹R. Penrose, *Bull. Inst. Math. Appl.* **10**, 266 (1974). See also, M. Gardner, *Sci. Am.* **236**, No. 1, 110 (1977); B. Grunbaum and G. C. Shepard, "Tilings and Patterns" (Freeman, San Francisco, to be published).

¹²K. Kim and E. A. Stern, *Phys. Rev. B* **23**, 3781 (1981).

¹³E. A. Stern, D. E. Sayers, and F. Lytle, *Phys. Rev. B* **11**, 4836 (1975).

¹⁴E. A. Stern, C. E. Bouldin, B. Von Roedern, and J. Azoulay, *Phys. Rev. B* **27**, 6557 (1983).

¹⁵E. A. Stern and S. M. Heald, in *Handbook on Synchrotron Radiation*, edited by D. E. Eastman, Y. Farge, and E. E. Koch (North-Holland, Amsterdam, 1980), Vol. 1, Chap. 10.

¹⁶A. D. I. Nicol, *Acta Crystallogr.* **6**, 285 (1953).

¹⁷G. Bunker and E. A. Stern, *Phys. Rev. Lett.* **52**, 1990 (1984).

¹⁸K. F. Kelton and T. W. Wu, *Appl. Phys. Lett.* **46**, 1059 (1985).

¹⁹C. L. Henley, unpublished.

²⁰M. Cooper and K. Robinson, *Acta Crystallogr.* **20**, 614 (1966).